

## Research Article

# Dose-Dependent Differentiation of Gamma-Irradiated Hazelnut Samples by Mid-Infrared Spectroscopy Coupled with Chemometrics

Ayca Dogan <sup>1</sup>, Mete Severcan <sup>2</sup>, and Feride Severcan <sup>3</sup>

<sup>1</sup>Department of Physiology, Faculty of Medicine, Altinbas University, Istanbul 34145, Turkey

<sup>2</sup>Department of Electrical and Electronics Engineering, Altinbas University, Istanbul 34145, Turkey

<sup>3</sup>Department of Biophysics, Faculty of Medicine, Altinbas University, Istanbul 34145, Turkey

Correspondence should be addressed to Ayca Dogan; [ayca.mollaoglu@altinbas.edu.tr](mailto:ayca.mollaoglu@altinbas.edu.tr)

Received 2 June 2020; Revised 19 October 2020; Accepted 25 October 2020; Published 7 November 2020

Academic Editor: Jose S. Camara

Copyright © 2020 Ayca Dogan et al. This is an open access article distributed under the Creative Commons Attribution License, which permits unrestricted use, distribution, and reproduction in any medium, provided the original work is properly cited.

Gamma irradiation is used as a food preservation method. It is known that high-dose irradiation causes several structural and functional damages. Therefore, the detection of high-dose irradiated food samples is a critical issue in international trade. The objective of this work is to evaluate the potential of Fourier transform infrared (FTIR) spectroscopy for the differentiation of  $\gamma$ -irradiated hazelnuts at higher doses (3 kGy and 10 kGy) from the lower (1.5 kGy) and nonirradiated ones using multivariate statistical analysis, namely, principal component analysis (PCA) and hierarchical cluster analysis (HCA). This study showed that high-dose irradiated hazelnut samples can be clearly differentiated from the low-dose irradiated samples using unsupervised methods based on the spectral differences. Furthermore, dose-dependent discrimination was also achieved. In conclusion, FTIR spectroscopy combined with multivariate statistical analysis has potential for the development of a reliable and fast methodology for separation of high-dose irradiated food samples.

## 1. Introduction

Hazelnut (*Corylus avellana* L.) has importance in human nutrition and health because of its unique fat (mainly oleic acid) and nonfat (protein, natural sterols, dietary fiber, tocopherols, and phenolic antioxidants) composition, which affects human health positively [1, 2]. The role of hazelnut in reducing the cardiovascular disease, diabetes, and cancer has been reported [3]. In addition to its protective health effects, it has also economic importance [4, 5]. Hazelnut and its processed products are used in food, pharmaceutical, and cosmetic industry [6]. They can also be added in various products as ingredients. One of the main problems in hazelnut industry is to keep quality maintenance during storage due to insect disinfection and food-borne pathogens [7]. Moreover, quality of nuts can be affected during the storage period due to the changes in the physiology and biochemistry of the nut after harvesting [8]. Therefore, clear

understanding of the physiological and biochemical changes of plants during the postharvest period will contribute to improve storage conditions and thus preserve the quality of food samples. To prevent the postharvest loss of hazelnut and other crops, food irradiation is recognized as an effective technology [9].

The application of ionizing radiation in food industry has been recognized as beneficial to improve the safety and quality of food by increasing hygienic quality and extending shelf life as a postharvest food preservation method. Albeit benefits of food irradiation and approvals from the Food and Drug Administration (FDA), consumer acceptance of irradiated food has been progressing slowly [10]. Public has some concerns about induced radioactivity, formation of toxic byproducts, and nutrient losses in food due to irradiation treatment [10].

Irradiation can lead to some structural, functional, and nutritional alterations in foods depending on the applied

dose [11]. It has been reported that irradiation may lead to the appearance of toxic chemical compounds due to secondary effects or generate volatile substances that can affect organoleptic properties of the final product. In addition, the components of foods are chemically altered to some extent after irradiation [12, 13]. In particular, some changes in protein and fat contents occur as ionizing radiation generates free radicals that may induce lipid peroxidation, colour, and odour alteration [14–16]. Therefore, convenient and reliable methods are required to detect irradiation and estimate the applied dose to prevent the lack of confidence. Various physical and chemical methods have been proposed for the identification of irradiation such as mass spectroscopy (MS), gas chromatography (GC), photo-stimulated luminescence (PSL), thermoluminescence (TL), and electron spin resonance (ESR) [17]. However, these methods are rather labor-intensive and expensive and provide limited information [18].

Fourier transform infrared (FTIR) spectroscopy has been applied widely in food research to characterize food components [19], detect different treatment effect to food such as heating and irradiation [13, 20], evaluate food quality [21], determine food fraud [22], and investigate food/packaging interactions [23]. FTIR spectroscopy has several advantages over other techniques. For example, it provides specific information about the studied system at the molecular level, which allows investigation on structure and composition of the material. It has potential to probe samples without disturbing molecular structure and integrity. It is fast, reproducible, easy to perform, and capable of simultaneously detecting multiple parameters, including biomolecules, ingredients, and chemicals. The FTIR spectrum consists of numerous characteristic spectral features, which are correlated with the molecules present in the sample. However, the spectra generally contain overlapped absorption bands, which make it difficult to interpret the spectra. Multivariate statistical analysis enables to extract information from complicated spectra of samples. Applications of IR spectroscopy on food research coupled with multivariate analyses have been described for the quantitative determination of compounds [24], detection and differentiation of bacteria in food [25], characterization and classification of oils [26], authentication [27], and differentiation [28] of food samples. Hierarchical cluster analysis (HCA) and principal components analysis (PCA) are two multivariate analyses that could be coupled with FTIR spectroscopy to facilitate robust and reliable extraction of information, biomarkers, and discrimination within and between samples [29].

In 1980, the FAO/IAEA/WHO Joint Expert Committee on Food Irradiation reported that irradiated food with a dose up to overall average dose of 10 kGy does not require further testing [30]. According to FDA's standards and regulations, the permissible dose for insect disinfestation is 1 kGy and for reduction of microbial load for elimination of pathogens is 5 kGy for nut, oil, seed, and dried fruits [31]. In a previous mid-infrared spectroscopic study, we did detailed spectral characterization studies and determined radiation-induced global structural and contextual changes in biomolecules of

hazelnut samples at two different radiation doses (1.5 kGy and 10 kGy) [13] and reported that irradiation at 10 kGy-induced molecular damages in hazelnut tissues.

In the present study, in order to contribute to the quality control mechanism used in food industry, we tested the power of mid-infrared spectroscopy coupled with chemometric analysis as a novel approach in dose-dependent differentiation of irradiated hazelnut samples from the nonirradiated ones. For this purpose, 1.5, 3, and 10 kGy irradiation were applied to hazelnuts. Hierarchical cluster analysis (HCA) and principal components analysis (PCA) were applied to the spectra.

## 2. Materials and Methods

**2.1. Sample Preparation for FTIR.** Hazelnut samples, which were not exposed to irradiation previously, were obtained from local producers and irradiated with the dose of 1.5, 3, and 10 kGy using gamma radiation from a cobalt-60 source (ISSLEDOVATELJ (Gamma-cell)) at the Turkey Atomic Energy Authority Food Irradiation Unit as described in detail by Dogan et al. [13].

Hazelnut samples ( $n = 8$ ) were cut into four pieces, three of which were irradiated with the doses 1.5, 3, and 10 kGy and the last one was used as control. To obtain nut tissue powder, all samples were ground and dried in a MAXI dry lyo freeze dryer for overnight. Then, the ground samples mixed with potassium bromide (KBr) in a 1/100 ratio. This powder was compressed into a thin KBr disk under a pressure of  $\sim 100 \text{ kg/cm}^2$  for 8 minutes for FTIR spectroscopic investigation. This process was repeated three times for each control and irradiated samples, and the average spectrum was obtained for each sample using OPUS Software Programme.

**2.2. FTIR Data Collection.** Infrared spectra were generated in absorbance mode using a BOMEM MB157 FTIR (The Michelson Series, Bomem, Inc., Quebec, Canada) spectrometer equipped with a DTGS (deuterated triglycine sulphate) detector. The sample compartment was continuously purged by dry air to reduce water vapor and carbon dioxide interference.

The FTIR spectra of samples were recorded in the  $4000\text{--}1000 \text{ cm}^{-1}$  region at room temperature. Each interferogram was collected by co-adding 400 scans at  $4 \text{ cm}^{-1}$  resolution. Three different KBr disks obtained from each sample were scanned. They revealed almost identical spectra. Then, a mean FTIR spectrum was obtained for each sample and these average spectra were used in further analysis.

**2.3. Data Preprocessing.** A spectral quality test was applied to all FTIR spectra. This test included tests for residual water vapor bands and the signal-to-noise ratio. All spectra that have passed these tests were subsequently unit vector normalized. Vector normalization was performed over the investigated spectral region of interest separately, namely, the  $4000\text{--}1000 \text{ cm}^{-1}$ ,  $3050\text{--}2800 \text{ cm}^{-1}$ , and  $1800\text{--}1000 \text{ cm}^{-1}$  regions, using "The Unscrambler X" software, version 10.3.

**2.4. Chemometrics.** In order to compare the spectra of hazelnut samples irradiated with different doses with those of the control samples in terms of some underlying structural differences, two multivariate molecular spectral analyses methods, HCA and PCA, were used.

**2.5. Hierarchical Cluster Analysis.** HCA calculates the similarities between the spectra of samples by using distance calculation and classification algorithms. The results are presented in the form of a dendrogram which shows clustering in two dimensions by graphical means. The measure of similarity is heterogeneity, where increasing heterogeneity corresponds to increasing dissimilarity. In our study, hierarchical cluster analysis was performed for the bands in the 4000–1000  $\text{cm}^{-1}$ , 3050–2800  $\text{cm}^{-1}$  and 1800–1000  $\text{cm}^{-1}$  regions. The analyses were performed on unit vector-normalized spectra. The heterogeneity calculations were done using Ward's algorithm [32]. Ward's algorithm clusters as much homogeneous objects as possible by combining the spectra that form a within-cluster variance with the smallest squared Euclidean distance [33].

**2.6. Principle Component Analysis.** PCA is used to reduce the dimensionality of the data by projecting the data using a linear transformation onto a new space consisting of orthogonal vectors. The transformation matrix consists of the eigenvectors of the autocorrelation matrix of the whole set of spectra [34]. For an FTIR spectral input, this corresponds to the reduction of hundreds of absorbance values at corresponding spectral wavenumbers into a single point in a low dimensional space. The coordinates are the principle components (PC), and the plot obtained is called the scores plot [35]. Each PC describes the variations among samples in decreasing order. Thus, the first principle component, i.e., PC-1 expresses most of the variance in the data, PC-2 expresses the second largest variance in the data, and so on. As a result, information about the class separation is obtained by clustering similar samples from the scores plot. An increase in the spatial separation between the two points in a scores plot corresponds to an increase in the dissimilarity between these two samples, i.e., the absorbance spectra in the case of FTIR spectra as the input. Since PCs are orthogonal to one another, their interpretation can be done independently.

In the current study, PCA were carried out for the 4000–1000  $\text{cm}^{-1}$ , 3050–2800  $\text{cm}^{-1}$ , and 1800–1000  $\text{cm}^{-1}$  bands as in the HCA. The analyses were performed on unit vector-normalized spectra. PCA was implemented using “The Unscrambler X” software, version 10.3. NIPALS (Nonlinear Iterative Partial Least Squares) algorithm was used with full cross validation.

### 3. Results and Discussion

In the current study, we focused on FTIR spectroscopy coupled with multivariate analysis, which is used to monitor the differentiation of hazelnut samples in response to gamma irradiation treatment. The power and sensitivity of FTIR spectroscopy together with a multivariate spectral

analysis, namely, cluster and principal component analyses, were tested. Figure 1 demonstrates average FTIR spectra for control and irradiated (1.5 kGy, 3 kGy, and 10 kGy) hazelnut samples in the 4000–1000  $\text{cm}^{-1}$  regions. As seen from these figures distinct spectral variations in the frequency, signal intensity, and peak area values are observed among the low- and high-dose irradiated and control hazelnut samples. Therefore, it can be clearly seen that intergroup variability is high.

Major spectral differences are observed particularly in the CH stretching region (3050–2800  $\text{cm}^{-1}$ ), where mainly lipid molecules contributed to the spectral pattern. The spectral variations in these regions are due to the changes in the absorbance bands from olefinic  $\text{C}=\text{CH}$  and asymmetric and symmetric  $\text{CH}_3$  and  $\text{CH}_2$  functional groups. Areas of these bands were dramatically decreased in 3 kGy and 10 kGy irradiated samples with respect to those of the control hazelnut spectrum. A similar behaviour in the decrease of band areas with irradiation is observed in the 1800–1000  $\text{cm}^{-1}$  region. In this region, the amide bands at 1652  $\text{cm}^{-1}$  and 1546  $\text{cm}^{-1}$  were assigned to protein amide  $\text{C}=\text{O}$  stretching and amide N–H bending vibration (60%) coupled to C–N stretching vibration (40%) mode of the polypeptide and protein backbone, respectively. In the same region, the absorption band at 1746  $\text{cm}^{-1}$  is due to  $\text{C}=\text{O}$  stretching vibration of ester groups in triacylglycerols and two bands at 1462  $\text{cm}^{-1}$  and 1378  $\text{cm}^{-1}$  corresponding to the CH absorption bending vibration of  $\text{CH}_2$  and  $\text{CH}_3$  groups, respectively [36, 37], are also lipid-related bands. The bands at 1462  $\text{cm}^{-1}$  are correlated to the content of fatty acid chains [38]. The variations in the absorption areas of the bands mentioned above indicated that irradiation processes lead to variation in the contents of lipid and protein molecules as also reported previously in detail by our group for low-dose (1.5 kGy) and high-dose (10 kGy) irradiated hazelnut samples. The present work aims to differentiate the irradiated (1.5 kGy, 3 kGy, and 10 kGy) and nonirradiated groups because of its importance in hazelnut trade and to determine the dose, which does not cause significant compositional changes in terms of hazelnut quality by using the power of infrared spectroscopy coupled with chemometrics. For this purpose, unsupervised multivariate analysis techniques namely HCA and PCA were performed.

The HCA results are demonstrated as dendrograms (Figure 2). The spectra for each irradiated and control sample were subjected to HCA using the information contained in the 4000–1000  $\text{cm}^{-1}$ , 3050–2800  $\text{cm}^{-1}$ , and 1800–1000  $\text{cm}^{-1}$  spectral regions in Figures 2(a)–2(c), respectively.

The results of HCA for the 4000–1000  $\text{cm}^{-1}$  region are shown as a dendrogram in Figure 2(a). As seen from the figure, there is a cluster of high-dose irradiated samples consisting of 3 kGy and 10 kGy samples. Control samples also form clusters with 1.5 kGy samples. Only two 3 kGy irradiated samples fall into these clusters. Similar results were also obtained for the cluster analysis performed in the 3050–2800  $\text{cm}^{-1}$  and 1800–1000  $\text{cm}^{-1}$  regions as shown in Figures 2(b) and 2(c). In the 3050–2800  $\text{cm}^{-1}$  region, two 3 kGy samples and one 10 kGy sample fall into the clusters

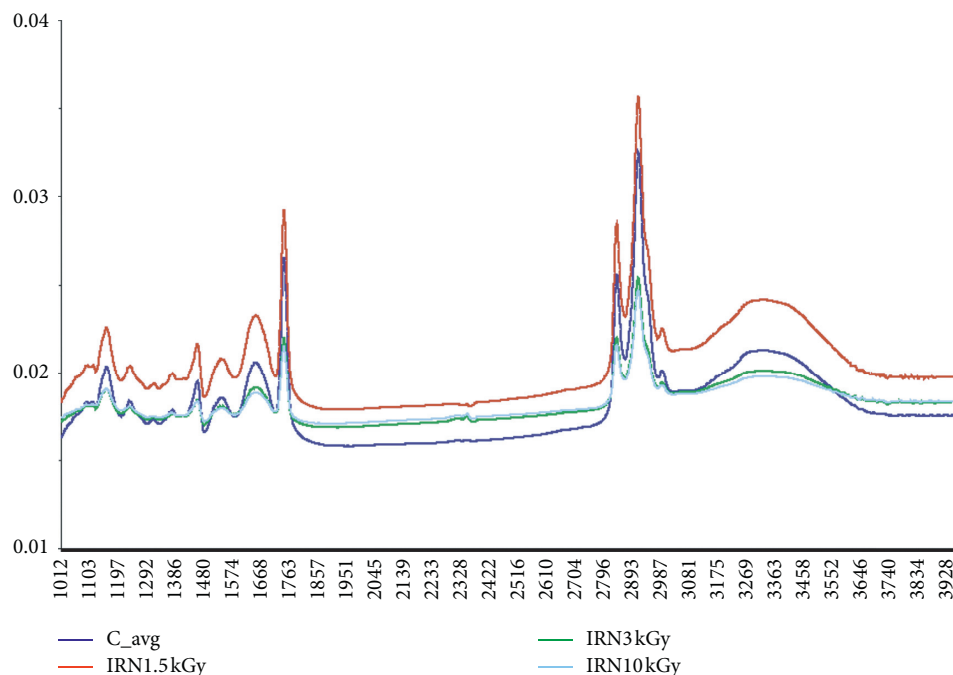


FIGURE 1: The average FTIR spectra of 1.5 kGy, 3 kGy, and 10 kGy irradiated and control hazelnut samples in the 4000–1000  $\text{cm}^{-1}$  region.

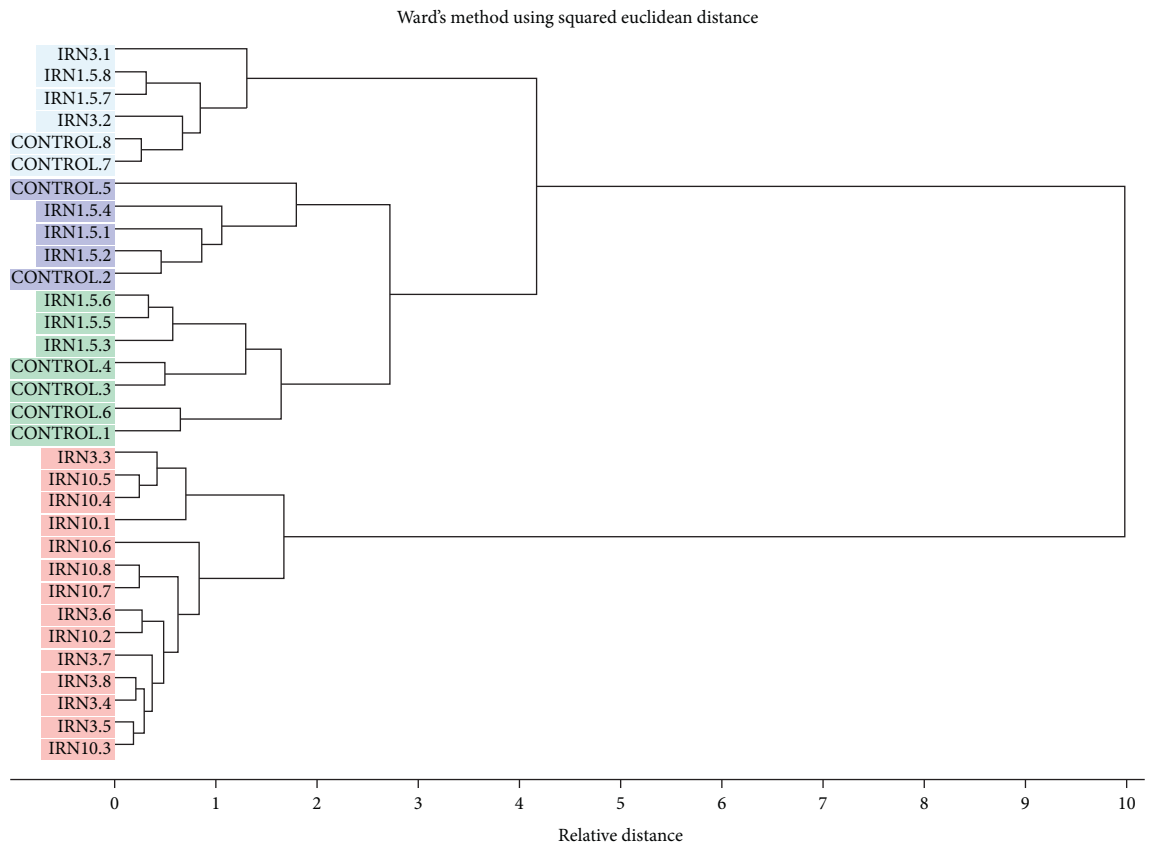
formed by control and low-dose irradiated samples. The results of HCA for the 1800–1000  $\text{cm}^{-1}$  region are similar to those of the whole region. The HCA results for all of the three regions analyzed indicate that the class of high-dose irradiated samples has a relatively high distance from the control plus low-dose irradiated groups. In addition, relative distance, or heterogeneity, within the high-dose irradiated group is much lower than the relative distances within control plus low-dose irradiated groups, implying that high-dose radiation removes sharp spectral differences due to the damages caused by high-level irradiation.

PCA results are shown as scatter plots (Figure 3). PCA was performed to demonstrate the capability of discrimination of high-dose irradiated hazelnut samples from control and low-dose irradiated samples. Figures 3(a)–3(c) show the score plots for the first two principle components PC-1 and PC-2 for three regions of the spectrum, namely, 4000–1000  $\text{cm}^{-1}$ , 3050–2800  $\text{cm}^{-1}$ , and 1800–1000  $\text{cm}^{-1}$  regions, respectively. These scatter plots should be considered as the projection of the multidimensional score values onto the first two axes (principal components). For all of the three regions analyzed, explained variance of the first two principal components is above 90%. It is obvious that there is a clear separation of high-dose classes from control class along PC-1. For the first two PCAs, control class has positive score values and 10 kGy irradiated samples have negative score values along PC-1, while for the 3rd PCA, the signs are opposite. In addition, the spread around the mean value of the scores of high-dose irradiated classes (3 kGy and 10 kGy) is much smaller than those of control and 1.5 kGy irradiated class. This is in agreement with the HCA results. Heterogeneity decreases as the radiation dose is increased. A measure of separation of classes is the Euclidean distance of the centroids (center of gravity) of the scores of samples in

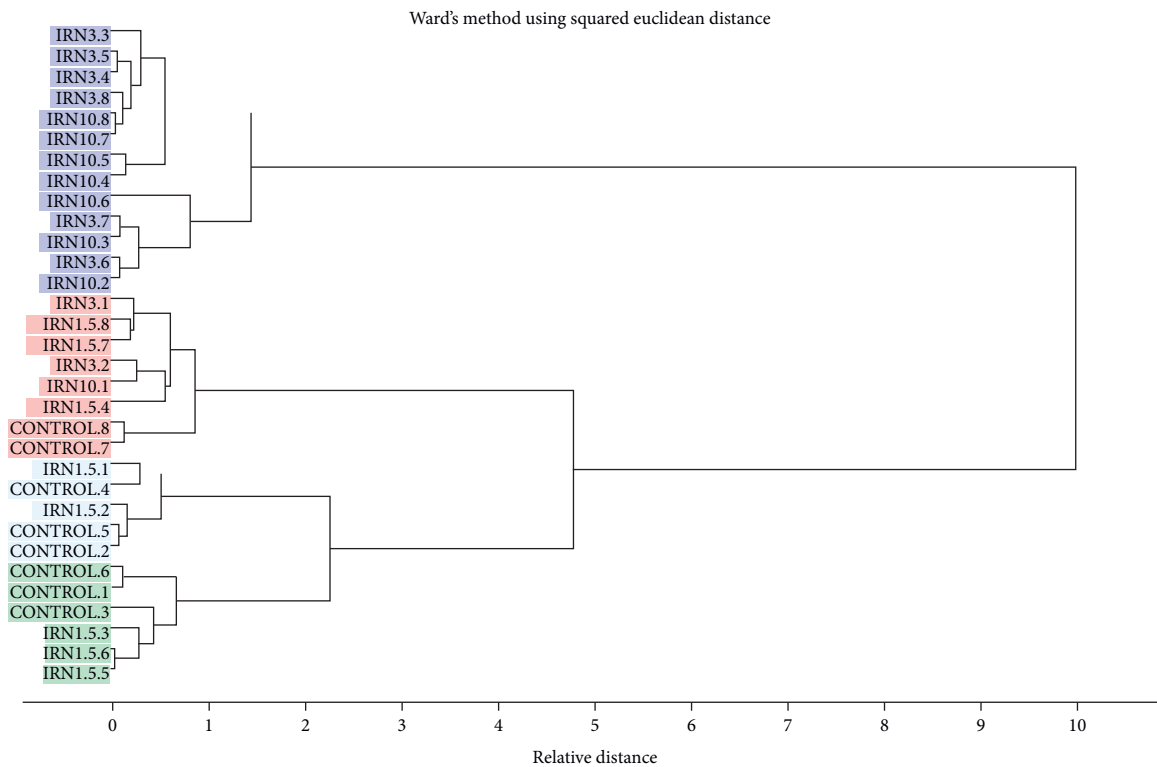
each class. Table 1 gives the distance of the centroids of 1.5 kGy, 3 kGy, and 10 kGy irradiated samples from the centroid of the scores of control samples. The distances were calculated using first 7 principal components. As observed from the PCA scores plots and from the calculated distances, 1.5 kGy irradiated samples are much closer to the control samples, and therefore, they are much less affected by irradiation.

PCA, in addition, provides information on the changes in the chemical composition of the samples at different irradiation levels. As an example, Figure 4 shows the loading plots (eigenvectors) for the first two principle components corresponding to Figure 3(c) (1800–1000  $\text{cm}^{-1}$  region). The loading plots of this region were given since it contains spectral bands belonging to almost all of the molecules in the system. For high-dose irradiated samples, PC-1 component scores are positive. Negative loading values in this case are an indication of a decrease in spectral values, for example, at wavenumbers 1747  $\text{cm}^{-1}$  and 1463  $\text{cm}^{-1}$ . Similar conclusions can be reached by looking at the loading curves at other regions of the spectrum.

Turkey has the world's leading position in the hazelnut sector by providing 70% of total production. Hazelnut has beneficial effects to human health due to its valuable oil (56–68%), protein (11–20%), and carbohydrate (10–22%) contents [3, 5]. Most of lipid contents are triacylglycerols and phospholipids. Saturated fatty acids (SFA), monounsaturated fatty acids (MUFA, which is mainly oleic acid), and polyunsaturated fatty acid (PUFA) contribute to fatty acid profile of hazelnut approximately as 6.63%, 82.45%, and 10.92%, respectively [29]. Free fatty acid content affects the quality and taste of hazelnuts [40]. It is known that radiation treatment can cause changes in the molecules depending on the applied dose level. Application of radiation generates



(a)



(b)

FIGURE 2: Continued.

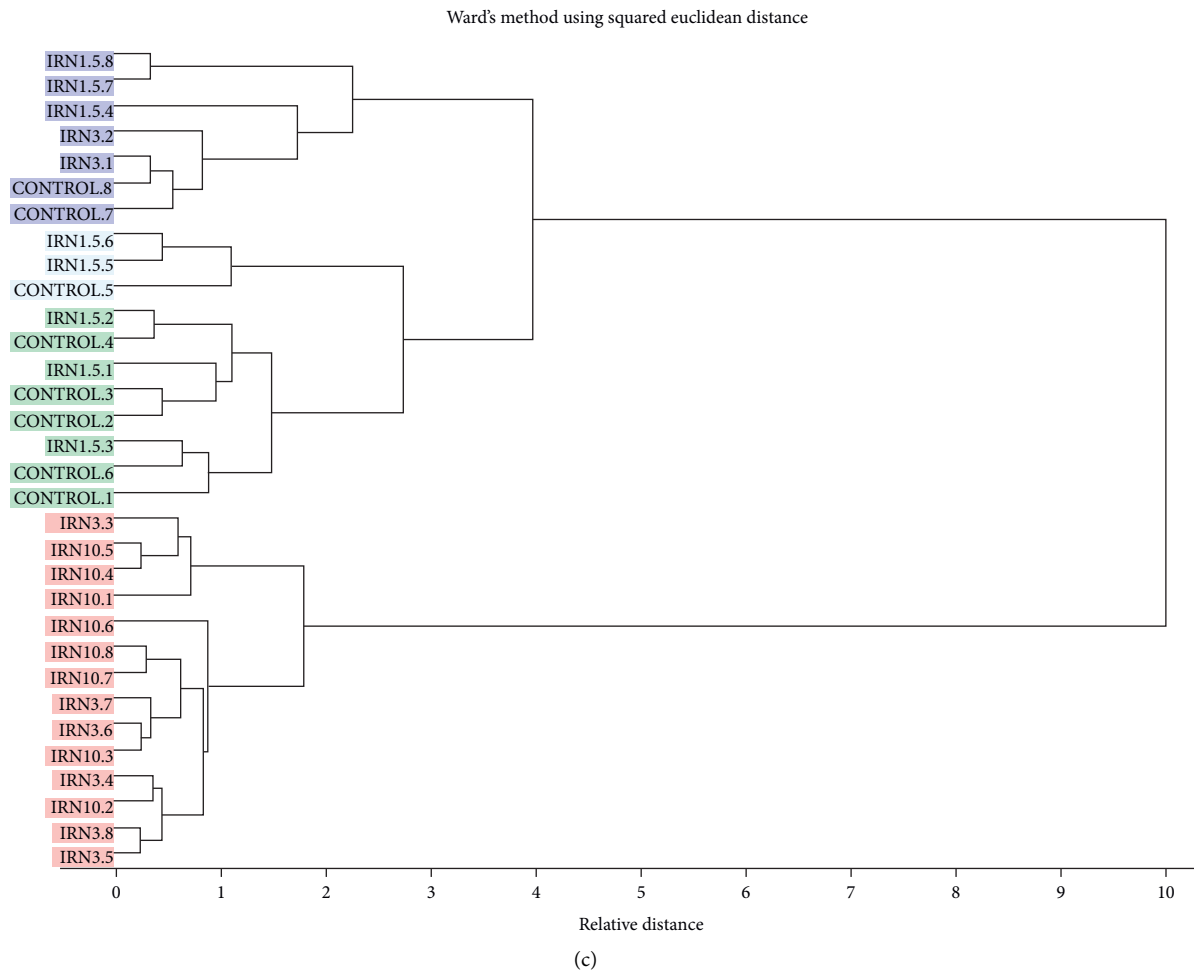


FIGURE 2: Hierarchical clustering of control and irradiated hazelnut groups using unit vector normalized spectra in the spectral range of (a) 4000–1000  $\text{cm}^{-1}$ , (b) 3050–2800  $\text{cm}^{-1}$ , and (c) 1800–1000  $\text{cm}^{-1}$ .

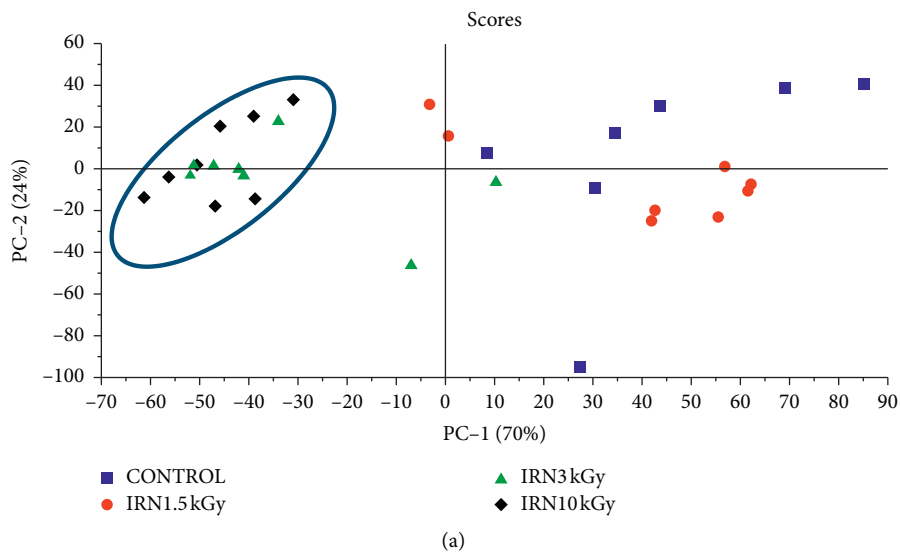


FIGURE 3: Continued.

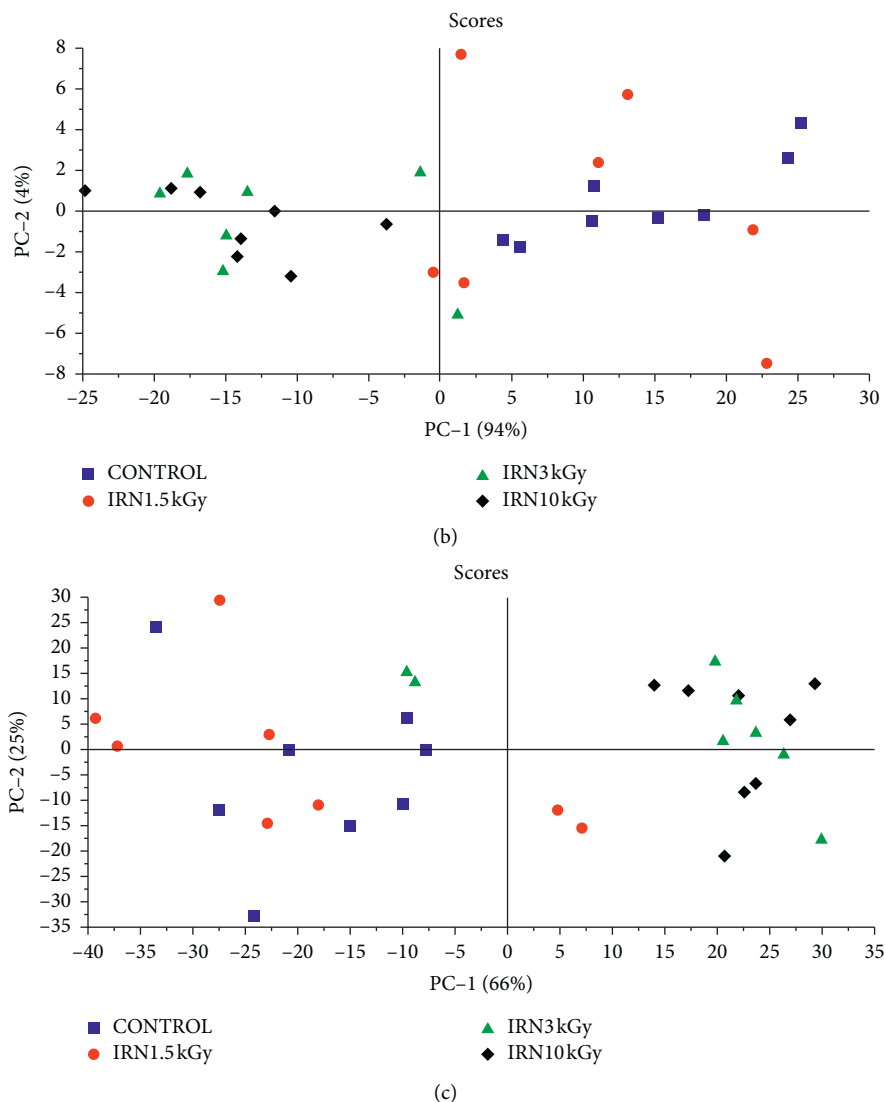


FIGURE 3: PCA score plots for control, 1.5 kGy irradiated, 3 kGy irradiated, and 10 kGy irradiated hazelnut samples in the (a) 4000–1000, (b) 3050–2800, and (c) 1800–1000  $\text{cm}^{-1}$  spectral regions.

TABLE 1: Distances of the centroids of 1.5 kGy, 3 kGy, and 10 kGy irradiated classes from the centroid of control samples.

Regions	Classes		
	IRN1.5 kGy	IRN3kGy	IRN10 kGy
4000–1000 $\text{cm}^{-1}$	31.1	77.7	90.5
3050–2800 $\text{cm}^{-1}$	12.2	28.7	31.3
1800–1000 $\text{cm}^{-1}$	17.6	38.1	43.7

hydroxyl radicals [41], which initiates lipid oxidation [42]. Particularly, nuts rich in unsaturated fatty acids are prone to oxidation when irradiated [14]. Furthermore, Golge and Ova [43] reported that irradiation leads to oxidation, decarboxylation, dehydration, and polymerization reactions, giving rise to lipid oxidation in fat molecules. This process also produces antioxidants, which can scavenge free radicals and esters, ketones, sulfur compounds, and aldehydes as a result of radiolysis [14]. On the other hand, it is known that

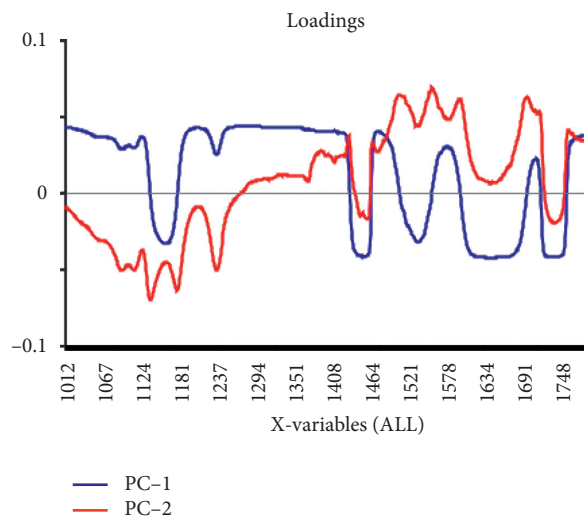


FIGURE 4: Loading plots for the first two PCs corresponding to the PCA in Figure 3(c).

not only lipid but also protein content is affected by irradiation treatment. In our previous study [13], we have reported that 10 kGy high-dose irradiation treatment leads to changes in the protein structure by decreasing the  $\alpha$ -helical structure and increasing the content of random coil that indicates aggregation and denaturation. Similar to our previous study, Guler et al. [44] have also reported that there was no difference in protein content between control and 1.5 kGy low-dose irradiation treatment, which supports our findings.

#### 4. Conclusions

Combination of ATR-FTIR spectroscopy with chemometric methods such as HCA and/or PCA successfully discriminate hazelnut samples according to the applied irradiation doses. The results revealed that 1.5 kGy irradiated samples cannot be discriminated from the control samples, indicating that irradiation at this dose did not significantly alter hazelnut composition and is suitable for irradiation of hazelnut samples. The alterations in the spectroscopic parameters such as signal intensity and frequency indicated that the irradiation process leads to global changes in the contents and structures of lipids and proteins. Based on these spectral changes, multivariate analyses provide robust and sensible methods for classification of irradiated samples. Both chemometric methods, HCA and PCA, have clustered the low- and high-dose irradiated samples independent from the chosen spectral region. The results of the present study revealed the capability of application of FTIR spectroscopy combined with multivariate analyses to make differentiation between low- and high-dose irradiated hazelnut samples. Present study is a demonstration of the applicability of the technique presented here, as a rapid, operator-independent, sensitive, and cost-effective technique in the field of food industry. Further studies using a larger number of samples will allow for the creation of a database and the adaptation of the mid-infrared spectroscopy for on-site application.

#### Data Availability

The data used to support the findings of this study are available from the corresponding author upon request.

#### Conflicts of Interest

The authors declare that there are no conflicts of interest regarding the publication of this paper.

#### Acknowledgments

The authors thank Galip Siyakus, Nurcan Cetinkaya, and Turkey Atomic Energy Authority Food Irradiation Unit (TAEK) for their support during the preparation of the irradiated hazelnut samples.

#### References

- [1] S. M. Mercanligil, P. Arslan, C. Alasalvar et al., "Effects of hazelnut-enriched diet on plasma cholesterol and lipoprotein profiles in hypercholesterolemic adult men," *European Journal of Clinical Nutrition*, vol. 61, no. 2, pp. 212–220, 2007.
- [2] D. Bagetta, A. Maruca, A. Lupia et al., "Mediterranean products as promising source of multi-target agents in the treatment of metabolic syndrome," *European Journal of Medicinal Chemistry*, vol. 186, p. 111903, 2020.
- [3] I. Oliveira, A. Sousa, J. S. Morais et al., "Chemical composition, and antioxidant and antimicrobial activities of three hazelnut (*Corylus avellana* L.) cultivars," *Food and Chemical Toxicology*, vol. 46, no. 5, pp. 1801–1807, 2008.
- [4] S. Gönenç, H. Tanrivermis, and M. Bülbül, "Economic assessment of hazelnut production and the importance of supply management approaches in Turkey," *Journal of Agriculture and Rural Development in the Tropics and Subtropics*, vol. 107, pp. 19–32, 2006.
- [5] A. İ. Köksal, N. Artik, A. Şimşek, and N. Günes, "Nutrient composition of hazelnut (*Corylus avellana* L.) varieties cultivated in Turkey," *Food Chemistry*, vol. 99, no. 3, pp. 509–515, 2006.
- [6] Anonymous, *Global Market Study on Hazelnut: Increasing Demand to Be Observed in the Pharmaceuticals Sector during 2018–2026*, <https://www.reportbuyer.com/product/5429853>, 2018.
- [7] M. Schmidt, E. Zannini, and E. K. Arendt, "Recent Advances in Physical Post-Harvest Treatments for Shelf-Life Extension of Cereal Crops," *Foods*, vol. 7, no. 4, 45 pages, 2018.
- [8] Deepshikha, B. Kumari, G. E. P. Devi, J. P. S. Sharma, S. Rawat, and J. P. Jaiswal, "Irradiation as an alternative method for post-harvest disease management: an overview," *International Journal of Agriculture, Environment and Biotechnology*, vol. 10, no. 5, p. 625, 2017.
- [9] J. Farkas and C. Mohácsi-Farkas, "History and future of food irradiation," *Trends in Food Science & Technology*, vol. 22, no. 2-3, pp. 121–126, 2011.
- [10] B. Maherani, F. Hossain, P. Criado et al., "World market development and consumer acceptance of irradiation technology," *Foods (Basel, Switzerland)*, vol. 5, no. 4, 79 pages, 2016.
- [11] F. Severcan and O. Bozkurt, "Application of vibrational spectroscopy to investigate radiation-induced changes in food," in *Applications of Vibrational Spectroscopy in Food Science*, pp. 241–259, Wiley, New York, USA, 2010.
- [12] C. Sommers and F. Xueting, *Food Irradiation: Research and Technology*, Blackwell Publishing Professional Ltd., Oxford, UK, 2006.
- [13] A. Dogan, G. Siyakus, and F. Severcan, "FTIR spectroscopic characterization of irradiated hazelnut (*Corylus avellana* L.)," *Food Chemistry*, vol. 100, no. 3, pp. 1106–1114, 2007.
- [14] S. F. Mexis and M. G. Kontominas, "Effect of  $\gamma$ -irradiation on the physicochemical and sensory properties of hazelnuts (*Corylus avellana* L.)," *Radiation Physics and Chemistry*, vol. 78, no. 6, pp. 407–413, 2009.
- [15] M. Al-Bachir, "Studies on the physicochemical characteristics of oil extracted from gamma irradiated pistachio (*Pistacia vera* L.)," *Food Chemistry*, vol. 167, pp. 175–179, 2015.
- [16] K. Liu, Y. Liu, and F. Chen, "Effect of gamma irradiation on the physicochemical properties and nutrient contents of peanut," *Lebensmittel-Wissenschaft & Technologie*, vol. 96, pp. 535–542, 2018.
- [17] J. Lee, T. Kausar, B.-K. Kim, and J.-H. Kwon, "Detection of  $\gamma$ -irradiated sesame seeds before and after roasting by analyzing photostimulated luminescence, thermoluminescence, and electron spin resonance," *Journal of Agricultural and Food Chemistry*, vol. 56, no. 16, pp. 7184–7188, 2008.



- [18] F. Verbeek, G. Koppen, B. Schaeken, and L. Verschaeve, "Automated detection of irradiated food with the comet assay," *Radiation Protection Dosimetry*, vol. 128, no. 4, pp. 421–426, 2008.
- [19] I. Dankar, A. Haddarah, F. E. L. Omar, M. Pujolà, and F. Sepulcre, "Characterization of food additive-potato starch complexes by FTIR and X-ray diffraction," *Food Chemistry*, vol. 260, pp. 7–12, 2018.
- [20] M. K. Grewal, T. Huppertz, and T. Vasiljevic, "FTIR fingerprinting of structural changes of milk proteins induced by heat treatment, deamidation and dephosphorylation," *Food Hydrocolloids*, vol. 80, pp. 160–167, 2018.
- [21] O. Anjos, A. J. A. Santos, L. M. Estevinho, and I. Caldeira, "FTIR-ATR spectroscopy applied to quality control of grape-derived spirits," *Food Chemistry*, vol. 205, pp. 28–35, 2016.
- [22] N. El Darra, H. N. Rajha, F. Saleh, R. Al-Oweini, R. G. Maroun, and N. Louka, "Food fraud detection in commercial pomegranate molasses syrups by UV-VIS spectroscopy, ATR-FTIR spectroscopy and HPLC methods," *Food Control*, vol. 78, pp. 132–137, 2017.
- [23] M. Mauricio-Iglesias, V. Guillard, N. Gontard, and S. Peyron, "Application of FTIR and Raman microspectroscopy to the study of food/packaging interactions," *Food Additives & Contaminants: Part A*, vol. 26, no. 11, pp. 1515–1523, 2009.
- [24] S. Abeysekara, D. Damiran, and P. Yu, "Univariate and multivariate molecular spectral analyses of lipid related molecular structural components in relation to nutrient profile in feed and food mixtures," *Spectrochimica Acta Part A: Molecular and Biomolecular Spectroscopy*, vol. 102, pp. 432–442, 2013.
- [25] B. Dziuba, A. Babuchowski, D. Nałęcz, and M. Niklewicz, "Identification of lactic acid bacteria using FTIR spectroscopy and cluster analysis," *International Dairy Journal*, vol. 17, no. 3, pp. 183–189, 2007.
- [26] M. Kharbach, R. Kamal, M. Bousrabat et al., "Characterization and classification of PGI Moroccan Argan oils based on their FTIR fingerprints and chemical composition," *Chemometrics and Intelligent Laboratory Systems*, vol. 162, pp. 182–190, 2017.
- [27] C. A. Nunes, "Vibrational spectroscopy and chemometrics to assess authenticity, adulteration and intrinsic quality parameters of edible oils and fats," *Food Research International*, vol. 60, pp. 255–261, 2014.
- [28] S. Gok, M. Severcan, E. Goormaghtigh, I. Kandemir, and F. Severcan, "Differentiation of anatolian honey samples from different botanical origins by ATR-FTIR spectroscopy using multivariate analysis," *Food Chemistry*, vol. 170, pp. 234–240, 2015.
- [29] F. Severcan and P. I. Haris, "Vibrational Spectroscopy in Diagnosis and Screening," *IOS Press*, vol. 6, pp. 16–17, 2012.
- [30] FAO/IAEA/WHO, Expert Committee, Wholesomeness of irradiated food, No: 659, WHO, Geneva, 1981.
- [31] M. H. Rahman, M. S. Islam, S. Begum et al., "Scientific opinion on the standards and regulations of irradiated food," *Journal of Nutrition & Food Sciences*, vol. 08, no. 04, 2018.
- [32] J. H. Ward, "Hierarchical grouping to optimize an objective function," *Journal of the American Statistical Association*, vol. 58, no. 301, pp. 236–244, 1963.
- [33] F. Severcan, O. Bozkurt, R. Gurbanov, and G. Gorgulu, "FT-IR spectroscopy in diagnosis of diabetes in rat animal model," *Journal of Biophotonics*, vol. 3, no. 8–9, pp. 621–631, 2010.
- [34] H. H. Nieuwoudt, B. A. Prior, I. S. Pretorius, M. Manley, and F. F. Bauer, "Principal component analysis applied to Fourier transform infrared spectroscopy for the design of calibration sets for glycerol prediction models in wine and for the detection and classification of outlier samples," *Journal of Agricultural And Food Chemistry*, vol. 52, no. 12, pp. 3726–3735, 2004.
- [35] T. Nakamura, J. G. Kelly, J. Trevisan et al., "Microspectroscopy of spectral biomarkers associated with human corneal stem cells," *Molecular Vision*, vol. 16, pp. 359–368, 2010.
- [36] Y. B. Che Man and G. Setiowaty, "Application of fourier transform infrared spectroscopy to determine free fatty acid contents in palm olein," *Food Chemistry*, vol. 66, no. 1, pp. 109–114, 1999.
- [37] M. D. Guillén and N. Cabo, "Usefulness of the frequency data of the Fourier transform infrared spectra to evaluate the degree of oxidation of edible oils," *Journal of Agricultural and Food Chemistry*, vol. 47, no. 2, pp. 709–719, 1999.
- [38] A.-M. Melin, A. Perromat, and G. Déléris, "Pharmacologic application of Fourier transform IR spectroscopy: In vivo toxicity of carbon tetrachloride on rat liver," *Biopolymers*, vol. 57, no. 3, pp. 160–168, 2000.
- [39] U. Gecgel, T. Gumus, M. Tasan, O. Daglioglu, and M. Arici, "Determination of fatty acid composition of  $\gamma$ -irradiated hazelnuts, walnuts, almonds, and pistachios," *Radiation Physics and Chemistry*, vol. 80, no. 4, pp. 578–581, 2011.
- [40] B. Ozyardimci, N. Cetinkaya, E. Denli, E. Ic, and M. Alabay, "Inhibition of egg and larval development of the Indian meal moth *Plodia interpunctella* (Hübner) and almond moth *Ephestia cautella* (Walker) by gamma radiation in decorticated hazelnuts," *Journal of Stored Products Research*, vol. 42, no. 2, pp. 183–196, 2006.
- [41] J. F. Diehl, C. Hasselmann, and D. Kilcast, "Regulation of food irradiation in the European Community: is nutrition an issue?" *Food Control*, vol. 2, no. 4, pp. 212–219, 1991.
- [42] E. J. Lee and D. U. Ahn, "Production of volatiles from fatty acids and oils by irradiation," *Journal of Food Science*, vol. 68, no. 1, pp. 70–75, 2003.
- [43] E. Gölgel and G. Ova, "The effects of food irradiation on quality of pine nut kernels," *Radiation Physics and Chemistry*, vol. 77, no. 3, pp. 365–369, 2008.
- [44] S. K. Guler, S. Z. Bostan, and A. H. Con, "Effects of gamma irradiation on chemical and sensory characteristics of natural hazelnut kernels," *Postharvest Biology and Technology*, vol. 123, pp. 12–21, 2017.